On the intuitive understanding of interrogating Fabry-Perot etalon with a focused beam

Dylan M. Marques, James A. Guggenheim, Rehman Ansari, Edward Z. Zhang, Paul C. Beard, et al.

Dylan M. Marques, James A. Guggenheim, Rehman Ansari, Edward Z. Zhang, Paul C. Beard, Peter R. T. Munro, "On the intuitive understanding of interrogating Fabry-Perot etalon with a focused beam," Proc. SPIE 10878, Photons Plus Ultrasound: Imaging and Sensing 2019, 108780Q (27 February 2019); doi: 10.1117/12.2508413

SPIE.

Event: SPIE BiOS, 2019, San Francisco, California, United States

On the intuitive understanding of interrogating Fabry-Perot etalon with a focused beam

Dylan M. Marques, James A. Guggenheim, Rehman Ansari, Edward Z. Zhang, Paul C. Beard, and Peter R. T. Munro

Department of Medical Physics and Biomedical Engineering, University College London, Gower Street, London WC1E 6BT, UK

ABSTRACT

Polymer film Fabry-Perot (FP) sensors are commonly used to detect ultrasound for Photoacoustic (PA) imaging providing high resolution 3D images. Such high image quality is possible due to their low Noise Equivalent Pressure (NEP) because of their broadband response and small acoustic element size. The acoustic element size is small (<100 µm) as defined, to first approximation, by the spot size of the focused interrogation beam. However, it has been difficult until now to gain an accurate intuitive understanding of the working principle of FP sensors interrogated with a focused beam. To overcome this limitation a highly realistic rigorous model of the FP sensor's optical response has used to establish a new intuitive understanding. The origin of fringe depth reduction and asymmetry associated with the FP sensors optical response is explained using the model developed.

Keywords: Fabry-Perot etalon, ultrasound sensor, all-optical detection, photoacoustic imaging, interferometer transfer function

1. INTRODUCTION

Photoacoustic (PA) imaging is a promising technique for medical imaging due its high spatial resolution (down to 50 µm), high penetration depth (up to a few centimetres) and high contrast based on optical absorption by tissue.[1] Some biomolecules such as haemoglobins or lipids heat their surroundings when illuminated with light, at specific wavelengths, leading to a generation of ultrasound waves. By recording these PA induced ultrasound waves with an array of sensors, a 3D map of the initial pressure distribution can be reconstructed.[2] One approach to detect the PA signal employs a system based on a Fabry-Perot (FP) etalon, which can provide a uniform frequency response (over 20 MHz) with a small acoustic element size defined by the interrogation optical spot size.[3] These features lead to high fidelity PA images with a penetration depth up to 1 cm.[4]

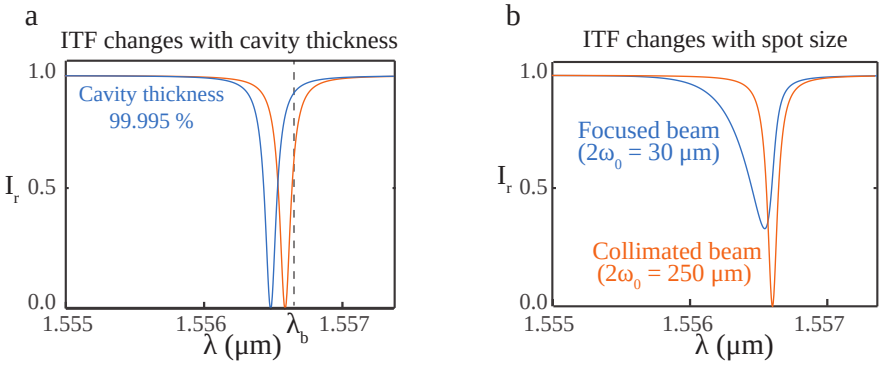

Figure 1. **a)** an example of a simulated ITF when the FP cavity of 38 µm is compressed by 0.005 %. **b)** Differences on the ITF shape when employing a focused beam ($2\omega_0$=30 µm) and an approximately collimated beam ($2\omega_0$=250 µm).

Further author information:
D.M.M.: E-mail: dylan.marques.17@ucl.ac.uk

Photons Plus Ultrasound: Imaging and Sensing 2019, edited by Alexander A. Oraevsky, Lihong V. Wang,
Proc. of SPIE Vol. 10878, 108780Q · © 2019 SPIE · CCC code: 1605-7422/19/$18 · doi: 10.1117/12.2508413

A FP etalon is an optical resonator made by a cavity formed between two mirrors. Ultrasound wavefronts are detected by sensing the power reflected by an FP etalon when a focused laser interrogation beam is incident upon it. The reflected power as a function of the interrogation laser wavelength is called the Interferometer Transfer Function (ITF) (see Fig. 1 a)). When the interrogation wavelength is near the resonance wavelength of the FP etalon, a rapid change in the reflected power occurs forming an interferometric fringe. Ultrasound waves perturb the optical thickness of the cavity thus changing the resonance wavelength. By monitoring the reflected power, the ultrasound waves are able to be detected. The ultrasound wavefront is spatially mapped in 2D by raster scanning the focused interrogation beam across the surface of the sensor.

The FP etalon sensitivity is the product of the acoustic and optical sensitivity: the former is related to how strongly an ultrasound wave changes the optical thickness of the cavity while the latter is related to how the power reflected by the sensor changes as the cavity thickness varies. The optical sensitivity is given by the ITF derivative at the operating interrogation wavelength. To maximize the optical sensitivity the wavelength is biased at the point that maximizes the ITF derivative (λ_b). Therefore, the ITF must be as sharp as possible to maximize the change in the reflected power as the optical path length inside the cavity changes. However, to keep the acoustic element size small, a focused interrogation beam is used which reduces the fringe sharpness and fringe depth and leads to an asymmetric ITF as Fig. 1 b) shows. These behaviours are observed experimentally and theoretically but no complete explanation has yet been provided.[5]

To understand why these features appear, the interaction between a focused beam and an FP etalon was studied using a highly realistic model. The model predicts how an arbitrary focused beam interacts with a stratified medium and was well validated for the experimental conditions used in PA imaging.[5]

2. MODEL

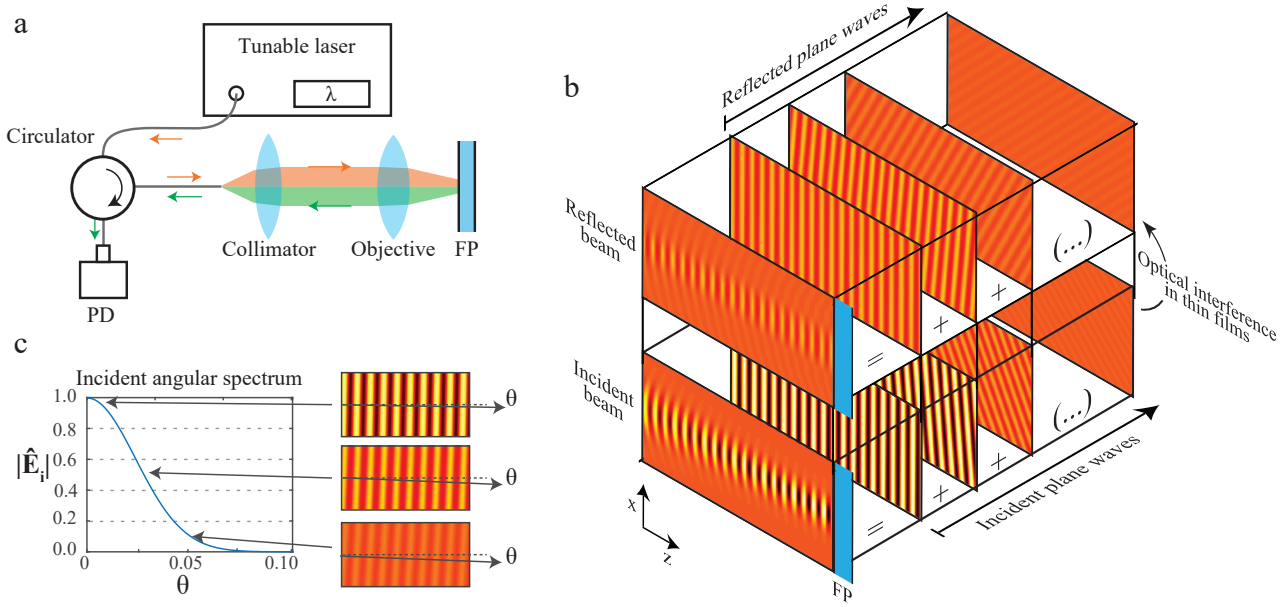

Figure 2. **a)** schematic of the setup modelled. **b)** schematic illustrating the principal components of the model. **c)** graphs showing the waveforms of representative plane wave components making up Gaussian beam with a spot size of $2\omega_0$=30 µm.

A typical optical optical setup used to readout an FP etalon is shown in Fig. 2 a).[3] Light is delivered from a tunable laser to a lens system by a single mode fibre which focuses the light onto the FP etalon surface. Light reflected from the FP etalon propagates back though the fibre and is measured by a photodetector.

An arbitrary monochromatic beam can be represented as a sum of plane waves of a given amplitude, phase and propagation direction, i.e. the so-called Angular Spectrum (AS).[6–9] Fig. 2 b) depicts a cross section of a Gaussian beam and its interpretation as a sum of plane waves. The amplitude of each plane wave as a function

of its polar angle θ is illustrated in Fig. 2 c). θ defines the plane wave direction of propagation and therefore the incident direction on the FP etalon.

The Maxwell equations are solved for a stratified medium with an incident plane wave by the theory of optical interference in thin films.[10] This theory allows for the amplitude and phase of the reflected wave to be calculated for the FP etalon for a particular incident plane wave as illustrated in Fig. 2 b). This approach leads to the reflected AS and by superimposing all such reflected plane waves, the reflected beam can be synthesised. Assuming a fibre based readout scheme, the measured intensity corresponds to the light coupled back into the fibre.

The model has been applied to predict the ITF. A very good agreement has been achieved with an average error below 5 % for most of the features measured.[5] The validation was performed for a range of spot sizes $2\omega_0$* between 30 µm to 250 µm and mirror reflectivities R between 97 % to 99.5 %.

3. INTUITIVE UNDERSTANDING

The model decomposes the focused interrogation beam into a sum of plane waves. Following the rationale underlying the model, to intuitively understand how a focused beam interacts with a FP etalon, the first step is to understand how a plane wave interacts with the FP etalon (Sec. 3.1). This plane wave rationale is then extended to consider a focused beam in Sec. 3.2.

3.1 Plane wave illumination

ITFs with plane wave illumination are usually modelled using the Airy function.[11] This predicts how a plane wave (i.e., a perfectly collimated beam) is reflected by an FP etalon. The Airy function predicts a very sharp fringe when using an FP etalon with very high mirror reflectivity as in Fig. 3 a). If a focused beam is used instead, the ITF has an asymmetric profile and the fringe depth is reduced creating a wider fringe as observed in Fig. 3 b).

The interaction of a plane wave with an FP etalon is based on the plane wave interaction with the mirrors (M_1 and M_2) and the plane wave propagation inside the cavity. When the incident plane wave interacts with the first mirror it is partially reflected and partially transmitted. The transmitted plane wave propagates through the cavity until the second mirror where it is again partially reflected and partially transmitted. The same rationale applies recursively to the reflected plane waves leading to an infinite number of round trips being made by partially reflected plane waves within the FP cavity.

The total reflected light is therefore composed of the sum of the first reflection (red in Fig. 3 c)) and the light released from inside the cavity after successive reflections (green in Fig. 3 c)). When the optical path length inside the cavity matches an integer number of the wavelength, the light inside the cavity is in resonance. This condition is achieved when:

$$2n_c h_c cos(\theta_c) = N\lambda, \tag{1}$$

where n_c and h_c are the refractive index and the thickness of the cavity, respectively. θ_c is the plane wave propagation direction inside the cavity which is related to θ (the incident angle of the plane wave incident on the FP etalon) by the Snell's law. N is an arbitrary positive integer.

In resonance, the light inside the cavity interferes constructively with itself, whilst interfering destructively with the light directly reflected when the incident light interacts with M_1 (i.e., ↗ + ∑ (↗)=0 in Fig. 3 c)). The reflected intensity measured at resonance thus decreases as observed in the ITF. Out of resonance the light inside the cavity interferes destructively, cancelling itself and therefore, light directly reflected when the incident light interacts with M_1 is largely unperturbed (i.e., ∑ (↗)=0 in Fig. 3 c)).

*$2\omega_0$ is the full width at $1/e^2$ of the Gaussian beam intensity

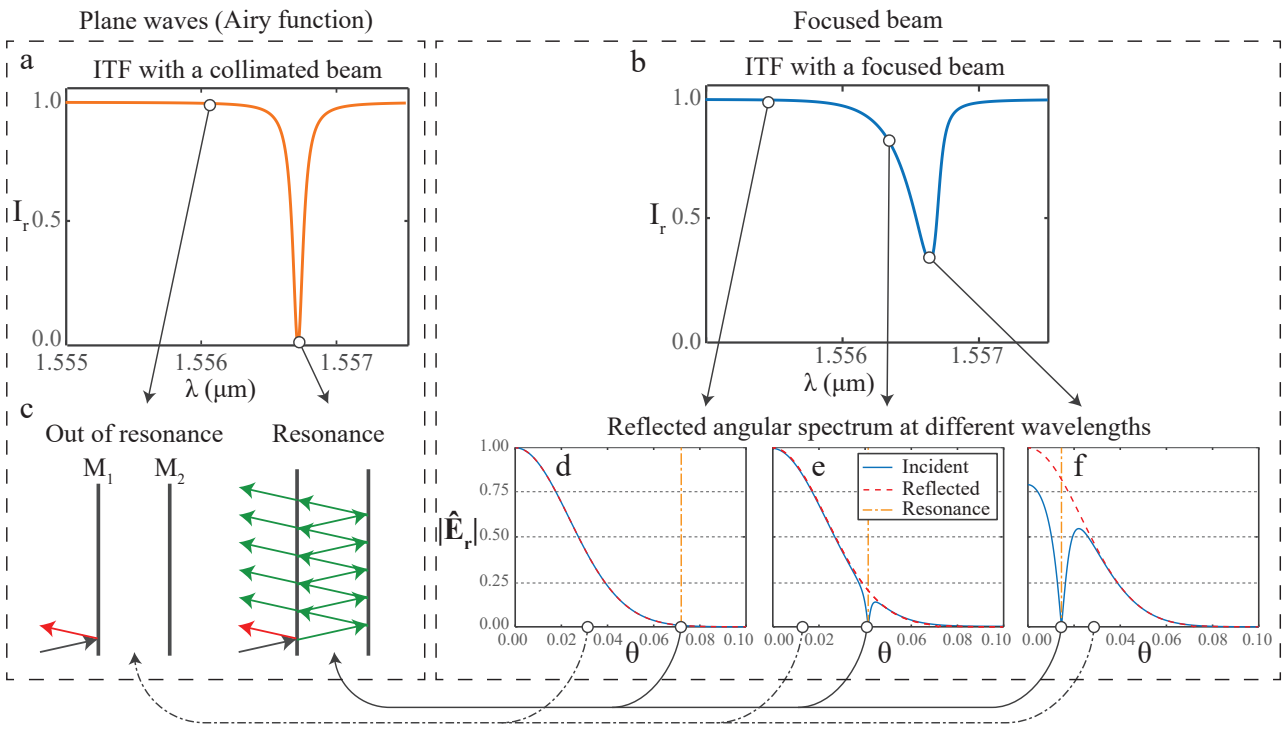

Figure 3. **a-b)** ITFs using a collimated beam ($2\omega_0$=250 µm) and a focused beam ($2\omega_0$=30 µm). **c)** schematic of the interaction between a plane wave and an FP etalon in resonance and out of resonance. **d-f)** incident and reflected angular spectrum at multiple wavelengths. The orange dashed line corresponds to the angle where the resonance condition is achieved (Eq. 1) for that specific wavelength.

3.2 Focused beam

When using a focusing interrogation beam, the ITF has an asymmetric profile and the fringe depth reduces as observed in Fig. 3 b). To understand how a focused beam is reflected from an FP etalon, a combination of the AS and the Airy function approaches is required. As explained in Sec. 2, the incident beam can be decomposed into a sum of plane waves each propagating with a different direction and therefore, incident on the FP etalon with a different angle. Each plane wave of the incident AS is reflected by the FP etalon as predicted by the Airy function.

Fig. 3 d-f) shows the reflected and incident AS at different wavelengths. Fig. 3 d) is at a wavelength in the flat region of the ITF and shows that all incident plane wave components are totally reflected. This is justified by the fact that any incident plane wave component is in the resonance condition (orange line). On the contrary, Fig. 3 e-f) shows that some of the incident plane wave components are not reflected since they are in resonance as predicted by the Airy function. However, some incident plane wave components do not achieve the resonance condition and are thus strongly reflected. When using a focused beam, even at the ITF minimum, only a subset of plane wave components are in resonance due to the spectrum of directions of propagation of the plane wave components. This leads to the reduction in the ITF depth since the plane wave components which are not in resonance are still detected.

Fig. 4 illustrates the origin of asymmetry in the ITF. At the ITF minimum the principal plane wave component is in resonance. Moving to shorter wavelengths the intensity change is less abrupt since the principal plane wave component is not in resonance but another plane wave achieved the resonance condition. Moving to longer wavelengths the intensity change is sharper since no plane wave component is in resonance. This is because the phase change per round trip within the cavity can only be decreased by increasing the plane wave angle of incidence. However, the optical path length can be reduced by increasing the angle of incidence.

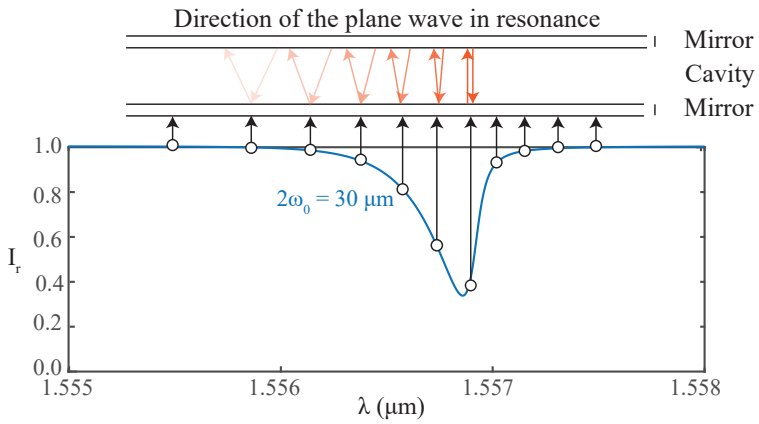

Figure 4. Schematic showing the direction of the plane wave in resonance at multiple wavelengths.

The analysis in this section shows that a focused interrogation beam reduces the FP sensor sensitivity due to the different optical paths inside the cavity resulting from the plane wave components having different directions of propagation. This phenomenon may be described as an angle dependent path length dispersion. In order to develop FP sensors interrogated by a focused beam with sensitivity comparable to when a collimated beam is used, the angle dependent path length dispersion must be corrected. This was achieved by Guggenheim et al. who developed a sensor with a plano-concave cavity that makes the optical path inside the cavity independent of the direction.[12]

4. CONCLUSION

Based on a full wave model of the interaction between a focused beam and a stratified medium, a new intuitive understanding of the physics behind interrogating an FP etalon with a focused beam was presented. The concept of angle dependent path length dispersion was introduced which reveals that only part of a focused interrogation beam's spectrum of plane waves is in resonance, which leads to a reduction in the sensitivity. Understanding the concept of angular phase dispersion will allow to development of novel and improved optical resonators.

ACKNOWLEDGMENTS

The authors acknowledge support from Engineering and Physical Sciences Research Council (EPSRC), European Research Council (ERC) and UCL Centre for Doctoral Training (CDT) for Medical Imaging. The authors P. R. T. Munro and J. A. Guggenheim are supported by Royal Society University Research Fellowships. D. M. Marques acknowledges the SPIE and MKS Instruments for the travel grant.

REFERENCES

[1] Beard, P., "Biomedical photoacoustic imaging," *Interface Focus* **1**(4), 602–631 (2011).

[2] Treeby, B. E. and Cox, B. T., "k-Wave: MATLAB toolbox for the simulation and reconstruction of photoacoustic wave fields," *Journal of Biomedical Optics* **15**(2), 021314 (2010).

[3] Zhang, E., Laufer, J., and Beard, P., "Backward-mode multiwavelength photoacoustic scanner using a planar Fabry-Perot polymer film ultrasound sensor for high-resolution three-dimensional imaging of biological tissues," *Applied Optics* **47**(4), 561 (2008).

[4] Jathoul, A. P., Laufer, J., Ogunlade, O., Treeby, B., Cox, B., Zhang, E., Johnson, P., Pizzey, A. R., Philip, B., Marafioti, T., Lythgoe, M. F., Pedley, R. B., Pule, M. a., and Beard, P., "Deep in vivo photoacoustic imaging of mammalian tissues using a tyrosinase-based genetic reporter," *Nature Photonics* **9**, 239–246 (mar 2015).

[5] Marques, D. M., Guggenheim, J. A., Ansari, R., Zhang, E. Z. Y., P. C. Beard, and Munro, P. R. T., "In preparation,".

[6] Foreman, M. R. and Török, P., "Computational methods in vectorial imaging," *Journal of Modern Optics* **58**(5-6), 339–364 (2011).
[7] Novotny, L. and Hecht, B., [*Principles of nano-optics*], Cambridge university press (2012).
[8] Wolf, E. and Richards, B., "Electromagnetic diffraction in optical systems," *Royal Society of London* , 349–357 (1959).
[9] Richards, B. and Wolf, E., "Electromagnetic Diffraction in Optical Systems II. Structure of the Image Field in an Aplanatic System," *Proceedings of the Royal Society A: Mathematical, Physical and Engineering Sciences* **253**(1274), 358–379 (1959).
[10] Fujiwara, H., [*Spectroscopic Ellipsometry: Principles and Applications*] (2007).
[11] Vaughan, M., [*The Fabry-Perot interferometer: history, theory, practice and applications*], Routledge (2017).
[12] Guggenheim, J. A., Li, J., Allen, T. J., Colchester, R. J., Noimark, S., Ogunlade, O., Parkin, I. P., Papakonstantinou, I., Desjardins, A. E., Zhang, E. Z., and Beard, P. C., "Ultrasensitive plano-concave optical microresonators for ultrasound sensing," *Nature Photonics* **11**(11), 714–719 (2017).